

# Population density estimated from locations of individuals on a passive detector array

MURRAY G. EFFORD,<sup>1,4</sup> DEANNA K. DAWSON,<sup>2</sup> AND DAVID L. BORCHERS<sup>3</sup>

<sup>1</sup>Zoology Department, University of Otago, P.O. Box 56, Dunedin, New Zealand

<sup>2</sup>USGS Patuxent Wildlife Research Center, 12100 Beech Forest Road, Laurel, Maryland 20708 USA

<sup>3</sup>Centre for Research into Ecological and Environmental Modelling, The Observatory, Buchanan Gardens, University of St Andrews, Fife KY16 9LZ Scotland

**Abstract.** The density of a closed population of animals occupying stable home ranges may be estimated from detections of individuals on an array of detectors, using newly developed methods for spatially explicit capture–recapture. Likelihood-based methods provide estimates for data from multi-catch traps or from devices that record presence without restricting animal movement (“proximity” detectors such as camera traps and hair snags). As originally proposed, these methods require multiple sampling intervals. We show that equally precise and unbiased estimates may be obtained from a single sampling interval, using only the spatial pattern of detections. This considerably extends the range of possible applications, and we illustrate the potential by estimating density from simulated detections of bird vocalizations on a microphone array. Acoustic detection can be defined as occurring when received signal strength exceeds a threshold. We suggest detection models for binary acoustic data, and for continuous data comprising measurements of all signals above the threshold. While binary data are often sufficient for density estimation, modeling signal strength improves precision when the microphone array is small.

**Key words:** *acoustic census methods; area search; camera trap; fecal DNA; maximum likelihood; microphone array; passive detector array; population density; proximity detector; signal strength; spatially explicit capture–recapture.*

## INTRODUCTION

Population density is a fundamental quantity in ecology, yet it is difficult to measure for many animal species. Species that are mobile or secretive are commonly sampled with passive detectors such as traps in a fixed spatial array. New technologies such as DNA sampling, digital photography, and digital sound recording, increase the list of species that can be surveyed with passive detectors. However, statistical analysis of passive detections is not straightforward because not all individuals are detected, and not all detected animals live within the perimeter of the array, resulting in both uncertainty about the area sampled and heterogeneity in the detection probabilities of individuals (we call these “edge effects”). Samples on two or more occasions can be analyzed by capture–recapture methods to estimate population size (e.g., Otis et al. 1978, Williams et al. 2002). When individuals are tagged or have natural marks, the data are a set of capture histories, each capture history being the temporal sequence of detection or non-detection for an individual. Although widely used, conventional capture–recapture

methods do not address the problems caused by edge effects.

Capture–recapture methodology has been extended recently to enable the fitting of a two-dimensional spatial point process for the central locations (loosely, “home-range centers”) of animals (Efford 2004, Borchers and Efford 2008, Royle and Young 2008). The key advantage of spatially explicit capture–recapture is that it provides direct estimates of population density unbiased by edge effects. The data are “spatiotemporal” capture histories, recording not just whether an individual was detected at a given time, but also the location (Fig. 1, Table 1).

Spatially explicit capture–recapture methods fit separate probability models for the distribution of animals (a spatial point process) and for the observation process. These methods require the probability model for sampling to be matched to the sampling device or “detector.” Efford (2004) and Borchers and Efford (2008) focused on traps as detectors; a trap yields no more than one detection for an individual in any sampling interval. Efford et al. (2009) and Royle et al. (2009) addressed “proximity” detectors, which do not trap individuals, but merely record their transient presence. Camera “traps” (a misnomer because the animal is not trapped) and hair snags for DNA sampling are commonly used forms of proximity detector. Although data from proximity detectors are slightly

Manuscript received 18 September 2008; revised 9 April 2009; accepted 12 May 2009. Corresponding Editor: D. C. Speirs.

<sup>4</sup> E-mail: murray.efford@otago.ac.nz

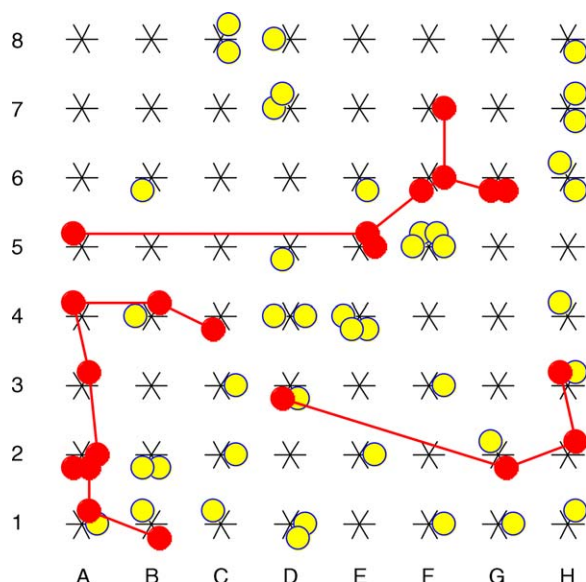


FIG. 1. Example of spatiotemporal detection data: 68 detections of 20 individuals over six sampling intervals simulated from a Poisson distribution of range centers (density  $D = 4.4 \text{ ha}^{-1}$ ) and a half-normal detection function (intercept  $g_0 = 0.1$ , spatial scale  $\sigma = 25.8 \text{ m}$ ), with grid spacing 20 m. Detections in successive intervals are depicted as radial “petals” clockwise from about five o’clock (petals may represent detections of more than one individual). The data for three individuals are highlighted for illustration (lines are a minimum-length tree). The full spatiotemporal history is used in the analyses described by Efford et al. (2009). This paper concerns “space-only” single-sample data that result when spatiotemporal histories are collapsed as shown in Table 1 for the upper highlighted individual, or from other single-sample spatial detection processes.

more complex than trapping data (because animals may be detected at multiple sites in one time interval), the analysis is simpler because detectors generally may be assumed to work independently. Software is available to estimate density by maximum likelihood from various detector types (e.g., Efford 2007).

We report an interesting feature of spatially explicit methods that was not recognized by Efford et al. (2009). Conventional capture–recapture methods require detections from multiple discrete occasions or time intervals (i.e., multiple samples), and this applies equally to spatially explicit capture–recapture from traps. However, density estimates may be obtained from spatial observations accumulated during just one time interval (i.e., a single sample) if each animal is potentially detected at multiple detectors, as is the case with proximity detectors. A single sample from one relatively long interval may be preferred over samples from multiple shorter intervals for reasons of economy or efficiency, and the possibility of analyzing a single spatial sample leads to entirely new applications.

The aim of this paper is to demonstrate single-sample spatially explicit capture–recapture methods, and to describe new models that are potentially useful for

single-sample data. A proximity detector as defined by Efford et al. (2009) generates binary data: animals are either observed or not observed at each detector. We propose two additional detector models that also allow multiple detections within a time interval, but that use non-binary data. The first is a “count proximity detector,” for which the data are the number of discrete observations for each animal/detector combination. The second is a “signal-strength proximity detector,” for which the data are a continuous measure that serves as a proxy for the distance between animals and detectors. An example is the intensity of a signal emitted by an animal and received by the detector. We specify probability models for each of these data types and evaluate their possible applications.

As an example, we consider the use of microphone arrays to assess the density of songbirds or whales from their vocalizations (Mellinger et al. 2007, Nichols et al. 2009). Each vocalization (e.g., bird song) is an ephemeral cue, distinguished from earlier and later cues by its approximately simultaneous arrival at the subset of microphones where it is detected. If cues from different individuals can be distinguished, estimation of cue density leads directly to an estimate of population density; otherwise, an estimate of the cue production rate is needed to convert cue density to population density (e.g., Buckland et al. 2001).

A sound can be sampled only once as it passes each detector, so a single-sample method is required to estimate cue density. The relative arrival times of a sound at different microphones may be used to localize the source, and cue density might be estimated using such localizations in combination with distance sampling (Buckland et al. 2001), although this has yet to be demonstrated (Mellinger et al. 2007). We present a simpler and possibly more rigorous approach: to bypass localization and estimate cue density directly from the spatial pattern of detections.

## METHODS

### Model and likelihood

We represent the general location of each individual in the population by the coordinates of a point that we call

TABLE 1. Collapsed spatiotemporal histories for the upper highlighted individual in Fig. 1.

Interval	Detector					
	A5	E5	F6	F7	G6	All other
1	0	0	0	0	1	0
2	0	0	1	0	1	0
3	0	0	0	0	0	0
4	1	0	0	0	0	0
5	0	1	0	0	0	0
6	0	1	1	1	0	0
Single sample						
Binary	1	1	1	1	1	0
Count	1	2	2	1	2	0

the animal's home-range center (hereafter "center"). Centers are fixed for the duration of the study, and the population is closed to births, deaths, immigration, and emigration. Probability of detection declines radially with increasing distance from the center, and the density of centers is the population parameter of interest. Centers are not observed directly. Each individual is detected at a set of sites, a footprint that we call its "detection pattern," or not at all. The set of  $n$  observed detection patterns provides the information needed to fit a two-dimensional distribution model, specifically an inhomogeneous Poisson process with rate parameter  $D$  (Borchers and Efford 2008).

Here we summarize the development of Borchers and Efford (2008) and Efford et al. (2009), as it applies for a single spatial sample. For  $K$  different detectors, each detection pattern is a vector of indicator values for the detection or non-detection of animal  $i$  at detectors  $1, \dots, K$  (we later extend the definition to include non-binary data). We use  $\omega$  for the set of all observed detection patterns. The joint likelihood of the detection parameters  $\theta$  and the point process parameters  $\phi$  is

$$L(\phi, \theta | n, \omega) = \Pr(n | \phi, \theta) \Pr(\omega | n, \phi, \theta) \quad (1)$$

which we dissect below. Estimation is by numerically maximizing the likelihood with respect to the parameters. We use asymptotic variance estimates from the inverse of the information matrix as these have previously been found to provide a fair approximation to more rigorous, but computationally expensive, profile likelihood estimates (e.g., Efford et al. 2009). Standard information-theoretic methods for model selection and model averaging apply (Burnham and Anderson 2002). Data augmentation and Markov chain Monte Carlo methods provide an alternative to likelihood maximization (Royle and Young 2008, Royle et al. 2009).

Borchers and Efford (2008) expressed the likelihood in terms of integrals over the real plane and approximated the integrals by summing over a set of  $M$  cells (a "habitat mask"). In this paper, we take the shortcut of including the summation in the likelihood. Each cell  $m$  has known area  $A$  and is centered at the  $x$ - $y$  coordinates given by the vector  $X_m$ . By discretizing the likelihood we fit a subtly different model (animals within a cell are treated as if they are massed at the center point, and density changes only at cell boundaries). Estimates will differ slightly from those of a continuous model, but the difference may be made arbitrarily small by reducing the cell size.

We assume that animals are located in space according to an inhomogeneous Poisson process with a rate  $D(X; \phi)$  per unit area at point  $X$ . If an animal at  $X$  is detected with probability  $p(X; \theta)$ , it follows that detected animals occur in space according to an inhomogeneous Poisson process with a rate  $D(X; \phi)p(X; \theta)$  per unit area at point  $X$ . For uniform habitat cells, it also follows that the probability of detecting  $n$  individuals (i.e., the factor  $\Pr(n | \phi, \theta)$  in Eq. 1) is obtained from a Poisson

distribution with rate parameter

$$\lambda(\phi, \theta) = A \sum_{m=1}^M D(X_m; \phi) p(X_m; \theta). \quad (2)$$

The other factor is obtained by rearranging expressions in Borchers and Efford (2008), collapsing the sampling intervals and using summation rather than integration:

$$\Pr(\omega | n, \phi, \theta) = A^n \lambda(\phi, \theta)^{-n} \prod_{i=1}^n \sum_{m=1}^M \prod_{k=1}^K \Pr(\omega_{ik} | X_m) D(X_m; \phi) \quad (3)$$

where  $\Pr(\omega_{ik} | X_m)$  is the probability of observing individual  $i$  at detector  $k$ . The second (nested) product assumes independence among detectors. We omit a constant binomial term that does not involve the parameters.

The density function  $D$  may take many different forms, possibly involving a trend over space or a response to habitat variables measured for each cell in the habitat mask. These details are not relevant to the rest of our paper, and  $D$  is constant in our examples (i.e., we fit a homogeneous Poisson process for centers).

#### Probability models for detection

Eqs. 2 and 3 include two quantities that we have yet to specify because their form depends on the detector type. These are the overall probability of detection  $p$ , and the probability of an observation at a particular detector  $\Pr(\omega_{ik} | X_m)$ . We provide expressions for these quantities for each of three possible detector types.

**Binary proximity model.**—For a binary proximity detector (Efford et al. 2009), the  $\omega_{ik}$  simply indicate detection (1) or nondetection (0) in a Bernoulli trial, and hence,

$$\Pr(\omega_{ik} | X_m) = p_k(X_m; \theta)^{\omega_{ik}} [1 - p_k(X_m; \theta)]^{1-\omega_{ik}} \quad (4)$$

where  $p_k(X_m; \theta)$  is the probability that an animal centered at  $X_m$  is detected at  $k$ , depending on  $\theta$ , a vector of parameters that we omit from here on, for clarity. In general,  $p_k$  is a decreasing function of the distance  $d_{km}$  between  $X_m$  and detector  $k$ :  $p_k(X_m) = g(d_{km}; \theta)$ , with intercept  $g(0) \leq 1.0$ . Particular forms for  $g$  that have been used successfully are the half-normal  $g(d) = g_0 \exp(-d^2/(2\sigma^2))$  with parameter vector  $\theta = (g_0, \sigma)$ , and the Hayes and Buckland (1983) "hazard-rate model"  $g(d) = g_0(1 - \exp(-(d/\sigma)^{-\tau}))$  with parameter vector  $\theta = (g_0, \sigma, \tau)$  (Efford et al. 2009). Overall detection probability follows directly:

$$p(X_m) = 1 - \prod_{k=1}^K [1 - p_k(X_m)]. \quad (5)$$

**Count proximity model.**—We define a count proximity detector as one for which each observation  $\omega_{ik}$  is a non-negative integer, a count of the times that animal  $i$  was detected at detector  $k$  within the sampling interval. Such

data might arise from photography over an extended period, or from collapsing binary detection data collected across multiple intervals. When the data result from collapsing  $N$  equal intervals, a binomial model is appropriate:

$$\Pr(\omega_{ik} | X_m) = \binom{N}{\omega_{ik}} p_k(X_m)^{\omega_{ik}} [1 - p_k(X_m)]^{N-\omega_{ik}} \quad (6)$$

and

$$p.(X_m) = 1 - \prod_{k=1}^K [1 - p_k(X_m)]^N. \quad (7)$$

This model is identical to that for data from multiple intervals when the probability of detection is constant (cf. Efford et al. 2009: Eqs. 3 and 4). Other possible distributions include Poisson and negative binomial (Appendix A). The binary proximity model (Eq. 4) is a limiting case of the binomial count model when  $N = 1$ . The models are distinct (i.e., binary data are not sufficient for the binomial model) when  $N > 1$  (Appendix A).

*Signal-strength model.*—We have assumed thus far that each observation  $\omega_{ik}$  is a discrete event, or a count of such events. We now extend the concept of detection to include the measurement of signals on a continuous scale. For example, a microphone coupled to a recorder registers signal attributes such as loudness, frequency composition, and distortion that provide information about the distance between the animal (the signal source) and the detector. We use the umbrella term “signal strength” for any measurable signal attribute that decreases with distance. The measure may be quite indirect: for example, a spectrogram cross-correlation value between a recording and a standard call, as commonly used for automated call recognition. It may be advantageous to include signal strength in the model even when there is no external calibration of signal strength in terms of distance (we test this idea below).

We assume a transformation  $h$  of signal strength  $S$  that declines linearly with distance  $d$  from the source:  $h(S) = \beta_0 + \beta_1 d + \epsilon$ , where  $\epsilon$  is normally distributed with mean zero and variance  $\sigma_\epsilon^2$ . If  $S$  takes positive real values then log transformation is appropriate; if  $S$  is constrained between 0 and 1, as with a cross-correlation score, then a logit transformation may be used. The model has three parameters: intercept  $\beta_0$ , slope  $\beta_1$ , and error variance  $\sigma_\epsilon^2$ .

The preceding model places no lower limit on the strength of signal that is detected. Very faint signals are prone to misidentification and their relative levels probably convey little useful information. We therefore impose an arbitrary threshold  $c$  of measured signal strength below which the record is censored. Noting that  $\omega_{ik}$  is the value of  $S$  for animal  $i$  at detector  $k$ , the probability that  $\omega_{ik}$  from an animal in cell  $m$  is less than  $c$  at detector  $k$  (i.e., that it is not detected by this detector) is  $\Phi(\gamma(X_m, k))$ , where  $\Phi$  is the standard normal

distribution function,  $\gamma(X_m, k) = (h(c) - \mu(X_m, k))/\sigma_s$ , and  $\mu$  is the expected value on the transformed scale ( $\mu(X_m, k) = \beta_0 + \beta_1 d_{km}$ ). The likelihood component associated with the signal from animal  $i$  at detector  $k$  is then

$$\Pr(\omega_{ik} | X_m) = \Phi(\gamma(X_m, k))^{1-\delta_{ik}} \times \left\{ (2\pi\sigma_s^2)^{-1/2} \exp\left(-[h(\omega_{ik}) - \mu(X_m, k)]^2 / (2\sigma_s^2)\right) \right\}^{\delta_{ik}} \quad (8)$$

where  $\delta_{ik}$  is an indicator variable for whether the observed signal strength  $\omega_{ik}$  exceeds  $c$  (or  $h(\omega_{ik}) > h(c)$ ) (e.g., Persson and Rootzén 1977). The probability that signal strength exceeds  $c$  at one or more detectors is

$$p.(X_m) = 1 - \prod_{k=1}^K 1 - \Phi(\gamma(X_m, k)). \quad (9)$$

### Simulations

We estimated density from simulated binary and count data to compare precision. In order to hold total effort constant, we first generated each realization from a binary proximity detector over six sampling intervals and then “collapsed” the time dimension to yield either single-sample count data or single-sample binary data (Fig. 1, Table 1). Parameter values were selected to yield realistic sample sizes (20, 50, or 100 individuals) and varying rates of recapture, by an algorithm described in Appendix B. Each simulated dataset was analyzed by fitting the binomial count and binary proximity models. See Appendix A for further details.

We also simulated an acoustic scenario in which songbirds were detected with a microphone array in a forest. A microphone is a “signal-strength proximity detector”: sound intensity, which can be measured from recordings, declines with distance and thus may be used as a distance proxy. Sound attenuation is measured on a logarithmic scale ( $S_{dB} = 10 \log_{10}(S/S_0)$ , where  $S_0$  is a reference level). At short range ( $< \sim 25$  m) sound attenuation in air is due mostly to spherical spreading ( $-6$  dB for each doubling of distance; Wiley and Richards 1982). At greater distances, other processes dominate that are more nearly linear on a log scale (e.g., atmospheric absorption, reflections from vegetation). For simplicity, we assumed attenuation to be linear on the decibel scale, although it is straightforward to include spherical spreading. We set  $\beta_0 = 70$  dB,  $\beta_1 = -0.3$  dB/m, and simulated two levels of error standard deviation ( $\sigma_s = 2.5$  dB,  $\sigma_s = 10$  dB) and two thresholds for censoring ( $c = -10, -30$  dB relative to  $\beta_0$ ). These values result in the detection–distance relationships in Fig. 2. Two microphone configurations were simulated: a single large array ( $10 \times 10$ ), and pooled data from 25 small arrays ( $2 \times 2$ ) operated independently. Microphones were 50 m apart. We compared density estimates under two models; in one



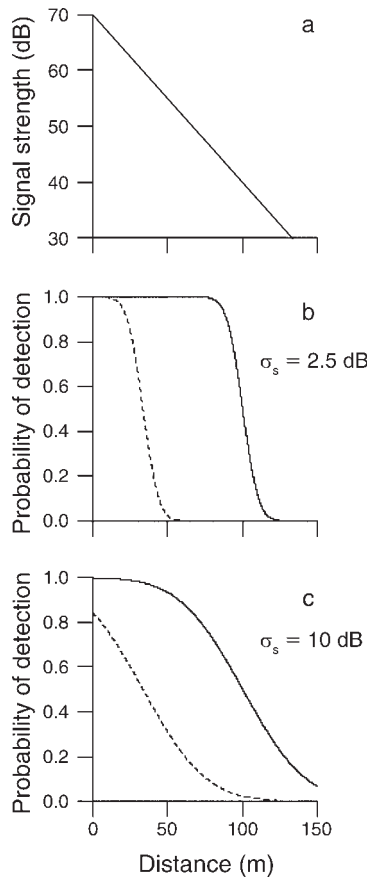


FIG. 2. Model for variation in detection probability resulting from linear signal attenuation with normal error SD  $= \sigma_s$ . Detection occurs when the signal at the detector exceeds an arbitrary threshold. (a) Expected signal strength from linear model  $S_{dB} = 70 - 0.3d$  dB. (b, c) Binomial detection probability for two levels of the detection threshold (40 dB, solid line; 60 dB, dashed line) and two levels of error.

the received signal strength above the detection threshold was modeled as a continuous variable (“signal-strength model”), and in the other detection was simply binary (“binary model”). Both models incorporated the binary detection model defined by  $\Pr(\omega_{ik} | X_m) = \Phi(y)^{1-\delta_{ik}} \{1 - \Phi(y)\}^{\delta_{ik}}$  (cf. Eq. 8), with  $p(X_m)$  as in Eq. 9. The linear attenuation parameters  $\beta_0$ ,  $\beta_1$ , and error standard deviation  $\sigma_s$  are confounded in the binary model, so we estimated the composite parameters  $(\beta_0 - c)/\sigma_s$  and  $\beta_1/\sigma_s$  (see Appendix C for details). The signal strength model additionally modeled variation among the detected signals, allowing  $\beta_0$ ,  $\beta_1$ , and  $\sigma_s$  to be estimated separately.

We used relative precision  $RSE(\hat{D})$  and relative bias  $RB(\hat{D})$  to summarize simulation results.  $RSE(\hat{D})$  is the estimated SE of the density estimate expressed as a percentage of the density estimate.  $RB(\hat{D})$  is the difference between the estimated and true density expressed as a percentage of the true density.

## RESULTS

Estimates of density from simulated binary and count data were generally similar and showed only a slight tendency to positive bias (Table 2). The estimated bias exceeded 10% only for one parameter combination with a low recapture rate ( $r/n = 0.4$ ), and then only under the binary model. Modeling binary data rather than counts caused very little loss of precision ( $\Delta RSE < 0.5\%$ ) except in the two scenarios with  $r/n < 1.0$ . Estimates of the detection parameters are given in Appendix A.

Both binary detection and signal-strength models fit to data generated with the signal-strength model yielded nearly unbiased estimates of population density (Table 3). Estimates of detection parameters ( $\beta_0$ ,  $\beta_1$ , and  $\sigma_s$  in the signal-strength model) were also generally unbiased, but even the “composite” parameters of the binary detection model could sometimes not be estimated with binary data collected on small arrays (Appendix C). The precision of density estimates was improved substantially by modeling signal strength when the microphone array was small, especially when signal variability ( $\sigma_s$ ) was low (Table 3). Asymptotic estimates of sampling variance were reliable for the scenarios we tested and, from a more limited set of trials, the coverage of the resulting 95% confidence intervals appears adequate (Appendix C).

## DISCUSSION

A single spatial sample from a passive detector array is sufficient for estimating the density of a closed population, providing detections can be attributed to individual animals. A single sample will be attractive where it is costly to visit detectors to collect samples from additional intervals and there is little risk of data loss from sample deterioration or device saturation. This is the case, for example, when polar bears (*Ursus maritimus*) are sampled using hair snags for DNA across hundreds of kilometers of arctic sea ice (P. J. van Coeverden de Groot, *personal communication*). Single-sample analytical methods also enable novel field designs. For example, a set of grid cells may be searched for fecal samples attributable to individual animals by analysis of microsatellite DNA (e.g., Taberlet and Luikart 1999). The counts of detections within a small grid cell may be modeled as if each detection occurred at the cell center; an additional factor for cell area  $A_c$  is included in the detection function (e.g.,  $g(d) = A_c g_0 \exp(-d^2/(2\sigma^2))$  for half-normal detection).

Density estimates from fitting a multi-sample binary model to the raw data were numerically identical to those from fitting a single-sample binomial model to the collapsed counts because both use the same binomial model, so we did not report them separately. Recaptures in space (the detection patterns in the single spatial sample) retain all necessary information on effective sampling area (Borchers and Efford 2008), and information from the temporal component of sampling is redundant. We do not know under what conditions, if

TABLE 2. Relative bias (RB) and precision (RSE) of spatially explicit estimates of population density from binary and binomial count models for varying expected number of first captures ( $n$ ) and recaptures ( $r$ ).

$n$	$r$	$r/n$	$g_0$	$\sigma$ (m)	$D$ (ha <sup>-1</sup> )	RB( $\hat{D}$ ) %		RSE( $\hat{D}$ ) %	
						Binary	Count	Binary	Count
20	20	1.0	0.1	15.0	7.4	3.3 (2.8)	4.4 (2.9)	26.2 (0.4)	25.9 (0.4)
20	50	2.5	0.1	25.8	4.4	5.2 (2.6)	5.2 (2.6)	24.2 (0.3)	24.1 (0.3)
20	100	5.0	0.1	50.8	1.9	-1.0 (2.7)	-1.6 (2.7)	28.6 (0.4)	28.4 (0.4)
50	20	0.4	0.1	9.5	32.1	11.5 (3.0)	4.4 (2.1)	27.8 (0.8)	20.8 (0.3)
50	50	1.0	0.1	15.0	18.5	1.5 (1.5)	1.0 (1.6)	15.8 (0.1)	15.6 (0.1)
50	100	2.0	0.1	22.2	12.6	1.1 (1.6)	1.1 (1.6)	15.2 (0.1)	15.1 (0.1)
100	50	0.5	0.1	10.6	55.5	2.4 (1.5)	-1.3 (1.3)	14.9 (0.2)	13.2 (0.1)
100	100	1.0	0.1	15.0	37.0	2.0 (1.1)	1.6 (1.1)	11.2 (0.1)	11.0 (0.1)
100	200	2.0	0.1	22.2	25.3	2.0 (1.1)	1.9 (1.1)	10.5 (0.1)	10.5 (0.1)

Notes: Simulated six-interval detection histories for an  $8 \times 8$  array of proximity detectors at 20-m spacing were collapsed to either binary or count single-interval detection patterns. Data were generated with a Poisson spatial distribution (density,  $D$ ) and half-normal detection model (parameters  $g_0$ ,  $\sigma$ ). Parameter values were selected to yield on average the given numbers of distinct individuals ( $n$ ) and recaptures ( $r$ ). A Poisson distribution model and half-normal detection model were fitted to the simulated data by maximum likelihood. Standard errors (in parentheses) are for 100 replicate simulations. RSE cannot be less than that for a Poisson distribution of  $n$  (22.4% when  $n = 20$ , 14.1% when  $n = 50$ , and 10.0% when  $n = 100$ ). See Appendix A for parameter estimates.

any, data on the temporal distribution of detections would improve estimation of closed population density. The question relates to the model used for the counts. A binomial count model assumes constant probability of detection over time, and approaches a Poisson model (Appendix A) for large  $N$  and small  $p$ . Some processes, such as a learned response to particular detector sites, will result in under- or over-dispersed counts (depending on whether the response is negative or positive). A negative binomial count model (Appendix A) may be used to accommodate overdispersion; A. Royle (*personal communication*) has suggested that this may be one scenario for which data from different intervals are useful.

A theoretical argument led us to expect some overall loss of precision in the density estimates when counts were reduced to a single-sample binary detection pattern (Appendix A). Our simulations show that in many cases the loss of precision is negligible. It is notable that the binary model is least adequate, in terms of both

precision and bias, when the counts (detections per individual per detector) are mostly 0 or 1 because there are few “recaptures” per individual ( $r/n < 1$ ).

Passive microphone arrays have been proposed for surveying animal abundance, both in the sea (Mellinger et al. 2007) and on land (e.g., Nichols et al. 2009), but it has been unclear how to analyze such data. The single-sample spatially explicit methods that we describe will allow biologists to obtain estimates of population density from passive acoustic data, without the need to localize individuals. This has great appeal as acoustic localization is technically demanding and generally possible for only a small fraction of the sounds detected (Mellinger et al. 2007; M. G. Efford and D. K. Dawson, *unpublished data*).

When a microphone array is small, estimation of the density of sound sources is substantially improved by modeling signal strength. This does not require external information on sound intensity at source or the relationship between signal strength and distance.

TABLE 3. Relative bias (RB) and precision (RSE) of cue density estimated from simulated acoustic signals by fitting a binary model or a signal strength model.

		RB( $\hat{D}$ )		RSE( $\hat{D}$ )	
$\sigma_s$ (dB)	$c$ (dB)	Binary	Signal strength	Binary	Signal strength
25 four-microphone arrays (data pooled)					
2.5	$\beta_0$ -30	-1.2 (1.1)	0.2 (0.7)	12.3 (0.3)	6.7 (0.02)
2.5	$\beta_0$ -10	4.4 (1.9)	3.0 (1.7)	17.9 (0.5)	16.5 (0.3)
10.0	$\beta_0$ -30	3.8 (2.0)	3.0 (1.6)	18.9 (0.4)	13.5 (0.2)
10.0	$\beta_0$ -10	5.5 (6.9)	-3.7 (3.0)	46.4 (3.4)	36.3 (2.6)
100-microphone array					
2.5	$\beta_0$ -30	0.9 (1.0)	0.8 (1.1)	11.0 (0.1)	11.0 (0.1)
2.5	$\beta_0$ -10	3.2 (1.6)	1.3 (1.4)	15.4 (0.2)	14.4 (0.1)
10.0	$\beta_0$ -30	2.4 (4.1)	-1.7 (1.0)	10.5 (0.1)	10.5 (0.1)
10.0	$\beta_0$ -10	-0.7 (1.2)	-0.7 (1.2)	13.5 (0.1)	13.5 (0.1)

Notes: Values are mean of 100 replicates (with SE in parentheses). Attenuation measured on a log scale was a linear function of distance (slope  $-0.3$  dB/m; Fig. 2). Received signal strength varied with a standard deviation of  $\sigma_s$ . The threshold of signal strength for detection  $c$  was  $-30$  dB or  $-10$  dB relative to signal strength at the source ( $\beta_0$ ). See Appendix C for estimates of attenuation parameters and other details.

Calibration is internal to each experiment, and uses the relative signal strength at known locations (microphones), much as detector spacing provides the spatial scale in the binary models. Small arrays have major advantages in the field: it is easier to position two microphones on a line or four microphones in a square than to set out a large grid, and we envisage multiple small arrays being located in a probability-based sampling design across a region of interest, as also advocated for distance sampling (Buckland et al. 2001). We report a field application elsewhere (D. K. Dawson and M. G. Efford, *unpublished manuscript*).

Models of received signal strength may have value even when there is little gain in the precision of density estimates. The separate parameters ( $\beta_0$ ,  $\beta_1$ , and  $\sigma_s$ ) are directly measurable in the field, opening the detection process to empirical investigation. If attenuation parameters can be estimated independently then their values may be fixed when maximizing the likelihood, potentially improving the precision of density estimates. Independent information on attenuation parameters may also be useful in forming priors for Bayesian analysis. Another possible application is in determining the appropriate grouping of species for analysis in multispecies studies.

#### ACKNOWLEDGMENTS

We thank Andy Royle, Tiago Marques, and two referees for their helpful comments on a draft of this paper.

#### LITERATURE CITED

- Borchers, D. L., and M. G. Efford. 2008. Spatially explicit maximum likelihood methods for capture–recapture studies. *Biometrics* 64:377–385.
- Buckland, S. T., D. R. Anderson, K. P. Burnham, J. L. Laake, D. L. Borchers, and L. Thomas. 2001. Introduction to distance sampling. Oxford University Press, Oxford, UK.
- Burnham, K. P., and D. R. Anderson. 2002. Model selection and multimodel inference: a practical information-theoretic approach. Second edition. Springer-Verlag, New York, New York, USA.
- Efford, M. G. 2004. Density estimation in live-trapping studies. *Oikos* 106:598–610.
- Efford, M. G. 2007. Density 4.1: software for spatially explicit capture–recapture. Department of Zoology, University of Otago, Dunedin, New Zealand.
- Efford, M. G., D. L. Borchers, and A. E. Byrom. 2009. Density estimation by spatially explicit capture–recapture: likelihood-based methods. Pages 255–269 in D. L. Thomson, E. G. Cooch, and M. J. Conroy, editors. Modeling demographic processes in marked populations. Springer, New York, New York, USA.
- Hayes, R. J., and S. T. Buckland. 1983. Radial-distance models for the line-transect method. *Biometrics* 39:29–42.
- Mellinger, D. K., K. M. Stafford, S. E. Moore, R. P. Dziak, and H. Matsumoto. 2007. An overview of fixed passive acoustic observation methods for cetaceans. *Oceanography* 20:36–45.
- Nichols, J. D., L. Thomas, and P. B. Conn. 2009. Inferences about landbird abundance from count data: recent advances and future directions. Pages 201–235 in D. L. Thomson, E. G. Cooch, and M. J. Conroy, editors. Modeling demographic processes in marked populations. Springer, New York, New York, USA.
- Otis, D. L., K. P. Burnham, G. C. White, and D. R. Anderson. 1978. Statistical inference from capture data on closed animal populations. *Wildlife Monographs* 62:1–135.
- Persson, T., and H. Rootzén. 1977. Simple and highly efficient estimators for a type I censored normal sample. *Biometrika* 64:123–128.
- Royle, J. A., J. D. Nichols, K. U. Karanth, and A. M. Gopalaswamy. 2009. A hierarchical model for estimating density in camera-trap studies. *Journal of Applied Ecology* 46:118–127.
- Royle, J. A., and K. V. Young. 2008. A hierarchical model for spatial capture–recapture data. *Ecology* 89:2281–2289.
- Taberlet, P., and G. Luikart. 1999. Non-invasive genetic sampling and individual identification. *Biological Journal of the Linnean Society* 68:41–55.
- Wiley, R. H., and D. G. Richards. 1982. Adaptations for acoustic communication in birds: sound transmission and signal detection. Pages 131–181 in D. E. Kroodsma, E. H. Miller, and H. Ouellet, editors. Acoustic communication in birds. Volume 1. Production, perception, and design features of sounds. Academic Press, New York, New York, USA.
- Williams, B. K., J. D. Nichols, and M. J. Conroy. 2002. Analysis and management of animal populations. Academic Press, San Diego, California, USA.

#### APPENDIX A

Spatially explicit population estimates from single and multiple samples (*Ecological Archives* E090-188-A1).

#### APPENDIX B

Method for designing spatial capture–recapture simulations with known expected counts (*Ecological Archives* E090-188-A2).

#### APPENDIX C

Simulations to compare spatially explicit population estimates from signal-strength and binary detection models (*Ecological Archives* E090-188-A3).